# On The Effect of Flow Direction on Mixed Convection Around Heated Circular Cylinder

**Dr. Jalal M. Jalil* , Qasim S. Mehdi * * & Mohammed A. Ahmed*****

Received on: 28/10/2008
Accepted on: 26/1/2009

## Abstract

A numerical investigation of laminar mixed convection around horizontal isothermal cylinder is presented. The free stream direction varies between the vertically upward (assisting flow) and vertically downward (opposing flow). The governing equation in terms of the stream function, vorticity and temperature are expressed in a body-fitted coordinate system and solved numerically by explicit method. Results are presented for Reynolds number from 20 to 300 with Grashof numbers from 0 to 120000. The Prandtl number was kept constant at 0.7. Correlation for the average Nusselt number around the cylinder in the forced and mixed convection regime is suggested. Comparison with previous theoretical and experimental results shows good agreement. It was established that the maximum heat transfer from cylinder occurs in case of assisting flow.

**Keywords**: Stream function-vorticity, time marching, mixed convection

## تأثير اتجاه الجريان على الحمل المختلط حول اسطوانة مسخنة

**الخلاصة**

أجريت دراسة عددية للحمل المختلط الطباقي حول اسطوانة أفقية ثابتة درجة الحرارة. اتجاه الجريان الحر يتغير من الأعلى (الجريان المساعد) إلى الأسفل (الجريان المعاق). استخدمت معادلات الدوامية-دالة الانسياب-درجة الحرارة بدلالة نظام مطابقة إحداثيات الجسم وقد حلت عدديا بطريقة التعاقب المفرط. تم استعرض النتائج لعدد رينولد من 20-300 وعدد كراشوف من 0-120000 . ثبت عدد برانتل عند 0.7 . تم اقتراح علاقات لمعدل عدد نسلت حول الاسطوانة لنظام الحمل القسري و المختلط. أظهرت المقارنات مع النتائج النظرية والعملية تطابق جيد. وقد تبين بوضوح إن اعلى انتقال حرارة من الاسطوانة هو لحالة الجريان المساعد.

* Electromechanical Engineering Department, University of Technology /Baghdad
**Mechanical Engineering Department, University of Technology /Baghdad
*** Mechanical Engineering Department, Engineering Collage, University of Anbar/ Anbar

## Nomenclature

| | | | |
|---|---|---|---|
| D | cylinder diameter | $\alpha$ | thermal diffusivity |
| g | gravity acceleration | $\alpha'$, $\beta'$, $\lambda'$, | transforming coefficient |
| Gr | Grashof number $((g.\beta.(T-T_w).D^3/\upsilon^2)$ | $\gamma'$ | thermal expansion coefficient |
| n | outer normal vector | $\beta$ | density of fluid |
| Nu | local Nusselt number ( h.D/k) | $\rho$ | viscosity of fluid |
| $\overline{Nu}$ | average Nusselt number ( $\overline{h}$.D/k) | $\mu$ | kinematic viscosity of fluid |
| $\overline{h}$ , h | local and average heat transfer coefficient | $\upsilon$ | dimensionless time |
| | | $\tau$ | free stream direction |
| IT | iteration | $\lambda$ | angular position |
| J | Jacobain of transformation | $\gamma$ | stream function |
| K | thermal conductivity | $\psi$ | dimensionless stream function |
| P | pressure | $\Psi$ | vorticity |
| Pr | Prandtl number ($\upsilon/\alpha$) | $\Omega$ | dimensionless vorticity |
| Pe | Peclte number (Re.Pr) | $\omega$ | dimensionless temperature |
| Re | Reynolds number ( $u_\infty$.D/ $\upsilon$) | $\theta$ | (( T - $T_\infty$ ) /( $T_w - T_\infty$ )) |
| t | time | | |
| T | fluid temperature | Subscripts | |
| $T_w$ | cylinder surface temperature | | grid points in direction of ($\zeta$ , $\eta$) |
| $T_\infty$ | inlet temperature | i , j | |
| u,v | velocity components | w | at the cylinder surface |
| U, V | dimensionless velocity components | o | at inlet |
| $u_\infty$ | velocity average | f | forced convection |
| x , y | physical coordinates | max | maximum value |
| X,Y | dimensionless x, y coordinates (X=x/D, Y=y/D) | $\infty$ | free stream |
| $\zeta$ , $\eta$ | general coordinates | | |
| | | n , n+1 | time step |

## Introduction

Due to the prominent importance of heat transfer in energy technology, several practical applications involving mixed convection from heated cylinder with various orientations continue to command substantial attention. These applications include heat exchangers. The first comprehensive experimental work on the effect of various parameters on the rate of heat transfer from a circular cylinder was carried out by Hatton [1]. In their work, heat transfer measurements were performed for Reynolds numbers up to 45 and Rayleigh numbers up to 10. Combined free and forced convection from the horizontal cylinders, at different angles of air flow direction, was experimentally invest igated by Oosthuizen and Madan [2]. Other experimental studies are found in References [3-5]. On the other hand, the influence of free stream direction on Mixed convection heat transfer from a circular cylinder was numerically investigated by Badr [6].The cylinder, which has an isothermal surface, is placed with its axis horizontal and normal to the oncoming flow. The free stream direction varies between the vertically upward (assisting flow) and the vertically downward (opposing flow) directions. The study was based on the solution of the full conservation equations of mass, momentum and energy. The study was limited to Reynolds numbers up to (Re = 40) and Grashof numbers of ($Gr = Re^2$). Other theoretical studies are found in References [6-19].The main objective of this work is to conduct a theoretical investigation of the effect of flow direction on the heat transfer process for Reynolds number up to 300 and Grashof number up to 120000. The study is based on the solution of full Navier-Stokes and energyequatio

## Mathematical Formulation

### Governing Equations

The problem considered in this study is a viscous incompressible, and laminar flow passing across heated cylinder as shown in Figure (1). The governing equations consist of full Navier-Stokes and energy equations formulated in terms of velocity, pressure, and temperature. Under the Boussinesq approximation [20], these equations are

$$\frac{\partial u}{\partial x}+\frac{\partial v}{\partial y}=0 \qquad \text{.....(1)}$$

$$\frac{\partial u}{\partial t}+u\frac{\partial u}{\partial x}+v\frac{\partial u}{\partial y}=u\left(\frac{\partial^2 u}{\partial x^2}+\frac{\partial^2 u}{\partial y^2}\right)-\frac{1}{r}\frac{\partial p}{\partial x}+gb(T-T_\infty)\cos l \qquad \text{…(2)}$$

$$\frac{\partial v}{\partial t}+u\frac{\partial v}{\partial x}+v\frac{\partial v}{\partial y}=u\left(\frac{\partial^2 v}{\partial x^2}+\frac{\partial^2 v}{\partial y^2}\right)-\frac{1}{r}\frac{\partial p}{\partial y}+gb(T-T_\infty)\sin l \qquad \text{….(3)}$$

$$\frac{\partial T}{\partial t}+u\frac{\partial T}{\partial x}+v\frac{\partial T}{\partial y}=a\left(\frac{\partial^2 T}{\partial x^2}+\frac{\partial^2 T}{\partial y^2}\right) \qquad \text{….(4)}$$

To eliminate pressure from the above equation, the vorticity-stream function method will be based on in the solution to obtain two equations are vorticity transport and stream function equations as follows:

$$\frac{\partial^2 \Psi}{\partial X^2}+\frac{\partial^2 \Psi}{\partial Y^2}=-w \qquad (5)$$

$$\frac{\partial w}{\partial t}+\frac{\partial \Psi}{\partial Y}\frac{\partial w}{\partial X}-\frac{\partial \Psi}{\partial X}\frac{\partial w}{\partial Y}=\frac{1}{\mathrm{Re}}\left(\frac{\partial^2 w}{\partial X^2}+\frac{\partial^2 w}{\partial Y^2}\right)+\frac{Gr}{\mathrm{Re}^2}\left(\frac{\partial q}{\partial X}\sin l-\frac{\partial q}{\partial Y}\cos l\right) \qquad (6)$$

$$\frac{\partial q}{\partial t}+\frac{\partial \Psi}{\partial Y}\frac{\partial q}{\partial X}-\frac{\partial \Psi}{\partial X}\frac{\partial q}{\partial Y}=\frac{1}{Pe}\left(\frac{\partial^2 q}{\partial X^2}+\frac{\partial^2 q}{\partial Y^2}\right) \qquad \text{… (7)}$$

The initial conditions are

$\Psi = \omega = \theta = 0$ in the region for t = ....(8)

The boundary conditions used for computations are given as follows: uniform inflow with $\omega = \theta = 0$ and stream function will be a function to the length of inlet. At The cylinder surface, $\Psi = 0$ and $\theta = 1$ while the vorticity on the cylinder surface will not be treated easily, since its value depends on the average of the velocity components on the cylinder, which is unknown until the end of calculations. At upper and lower boundaries, $\omega = 0$ and $\theta_y = 0$. Also, stream function at upper boundary and lower boundary are($\Psi = 1$ and $\Psi = -1$) respectively. At outlet flow, $\Psi_x = \omega_x = \theta_x = 0$.

### Coordinate Transformation

Due to curvilinear geometry of the boundary, a system of general coordinate has been adopted here in order to obtain a computationally convenient representation of the physical domain. If x and y are set as physical domain and ζ and η as computational domain, then the computational domain can be specified by the following rectangle region

$0 \le \zeta \le 1$ , $0 \le \eta \le 1$.

The relationships of x , y and ζ , η for the present study are as follows

$\zeta = \zeta(x, y)$ …(9)

$\eta = \eta(x, y)$ …. (10)

With the above, the governing equations in computational domain are expressed as

$$\left(l'.\frac{\partial \Psi}{\partial z}+s'.\frac{\partial \Psi}{\partial h}+a'.\frac{\partial^2 \Psi}{\partial z^2}-2b'.\frac{\partial^2 \Psi}{\partial z \partial h}+g'.\frac{\partial^2 \Psi}{\partial h^2}\right)/J^2=-w \qquad \text{…(11)}$$

$$\frac{\partial w}{\partial t}+\frac{1}{J}\left(\frac{\partial \Psi}{\partial z}.\frac{\partial w}{\partial h}+\frac{\partial \Psi}{\partial h}.\frac{\partial w}{\partial z}\right)=\frac{1}{(J^2.\mathrm{Re})}\left(l'.\frac{\partial \Psi}{\partial z}+s'.\frac{\partial \Psi}{\partial h}+a'.\frac{\partial^2 \Psi}{\partial z^2}-2b'.\frac{\partial^2 \Psi}{\partial z \partial h}+g'.\frac{\partial^2 \Psi}{\partial h^2}\right)+\left(\frac{Gr}{\mathrm{Re}^2}\right)\left(\left(\frac{\partial q}{\partial z}.\frac{\partial Y}{\partial h}+\frac{\partial q}{\partial h}.\frac{\partial Y}{\partial z}\right)\sin l-\left(\frac{\partial q}{\partial h}.\frac{\partial X}{\partial h}-\frac{\partial q}{\partial z}.\frac{\partial X}{\partial h}\right)\cos l\right)/J \qquad \text{.. (12)}$$

$$\frac{\partial q}{\partial t}+\left(-\frac{\partial \Psi}{\partial z}.\frac{\partial q}{\partial h}+\frac{\partial \Psi}{\partial h}.\frac{\partial q}{\partial z}\right)/J=\left(l'.\frac{\partial q}{\partial z}+s'.\frac{\partial q}{\partial h}+a'.\frac{\partial^2 q}{\partial z^2}-2b'.\frac{\partial^2 q}{\partial z \partial h}+g'.\frac{\partial^2 q}{\partial h^2}\right)/(J^2.Pe) \qquad \text{… (13)}$$

Where,

$$a' = x_h^2 + y_h^2$$

$$b' = x_z\, x_h + y_z\, y_h$$

$$g' = x_z^2 + y_z^2$$

$$l' = \left(x_h\, D_y - y_h\, D_x\right)/J$$

$$s' = \left(x_z\, D_x - y_z\, D_y\right)/J$$

$$D_x = a'\, x_{zz} - 2b'\, x_{zh} + g'\, x_{hh}$$

$$D_y = a'\, y_{zz} - 2b'\, y_{zh} + g'\, y_{hh}$$

### Method Of Solution

The two equations of vorticity transport and energy will be solved by explicit method finite difference based on the time marching technique. The time marching technique used for solving the unsteady governing equations to obtain the steady velocity and temperature distributions is based on studying the time development of the velocity and thermal fields

until reaching steady conditions. These equations are

$$w_{(i,j)}^{n+1}=w_{(i,j)}^{n}+\Delta t\left[\left(\frac{\Psi_{(i+1,j)}-\Psi_{(i-1,j)}}{2\Delta x}\cdot\frac{w_{(i,j+1)}^{n}-w_{(i,j-1)}^{n}}{2\Delta h}-\frac{\Psi_{(i,j+1)}-\Psi_{(i,j-1)}}{2\Delta h}\cdot\frac{w_{(i+1,j)}^{n}-w_{(i-1,j)}^{n}}{2\Delta x}\right)\Big/J_{(i,j)}+\left(l'_{(i,j)}\cdot\frac{w_{(i+1,j)}^{n}-w_{(i-1,j)}^{n}}{2\Delta x}+s'_{(i,j)}\cdot\frac{w_{(i,j+1)}^{n}-w_{(i,j-1)}^{n}}{2\Delta h}\right.$$

$$\left.+a'_{(i,j)}\cdot\frac{w_{(i+1,j)}^{n}-2w_{(i,j)}^{n}+w_{(i-1,j)}^{n}}{\Delta x^{2}}-2b'_{(i,j)}\cdot\frac{w_{(i+1,j+1)}^{n}-w_{(i+1,j-1)}^{n}-w_{(i-1,j+1)}^{n}+w_{(i-1,j-1)}^{n}}{4\Delta x\Delta h}\right.$$

$$\left.-\frac{q_{(i,j+1)}^{n}-q_{(i,j-1)}^{n}}{2\Delta h}\cdot\frac{Y_{(i+1,j)}-Y_{(i-1,j)}}{2\Delta x}\right)\frac{\sin l}{J_{(i,j)}}-\left(\frac{q_{(i,j+1)}^{n}-q_{(i,j-1)}^{n}}{2\Delta h}\cdot\frac{X_{(i+1,j)}-X_{(i-1,j)}}{2\Delta x}\right.$$

$$\left.-\frac{q_{(i+1,j)}^{n}-q_{(i-1,j)}^{n}}{2\Delta x}\cdot\frac{X_{(i,j+1)}-X_{(i,j-1)}}{2\Delta h}\right)\cdot\frac{\cos l}{J_{(i,j)}}\Bigg] \quad \ldots..(14)$$

$$q_{(i,j)}^{n+1}=q_{(i,j)}^{n}+\Delta t\left[\left(\frac{\Psi_{(i+1,j)}-\Psi_{(i-1,j)}}{2\Delta x}\cdot\frac{q_{(i,j+1)}^{n}-q_{(i,j-1)}^{n}}{2\Delta h}-\frac{\Psi_{(i,j+1)}-\Psi_{(i,j-1)}}{2\Delta h}\cdot\frac{q_{(i+1,j)}^{n}-q_{(i-1,j)}^{n}}{2\Delta x}\right)\Big/J_{(i,j)}+\left(l'_{(i,j)}\cdot\frac{q_{(i+1,j)}^{n}-q_{(i-1,j)}^{n}}{2\Delta x}+s'_{(i,j)}\cdot\frac{q_{(i,j+1)}^{n}-q_{(i,j-1)}^{n}}{2\Delta h}\right.\right.$$

$$\left.+a'_{(i,j)}\cdot\frac{q_{(i+1,j)}^{n}-2q_{(i,j)}^{n}+q_{(i-1,j)}^{n}}{\Delta x^{2}}-2b'_{(i,j)}\cdot\frac{q_{(i+1,j+1)}^{n}-q_{(i+1,j-1)}^{n}-q_{(i-1,j+1)}^{n}+q_{(i-1,j-1)}^{n}}{4\Delta x.\Delta h}\right.$$

$$\left.\left.+g'_{(i,j)}\cdot\frac{w_{(i,j+1)}^{n}-2.w_{(i,j)}^{n}+w_{(i,j-1)}^{n}}{\Delta h^{2}}\right)\Big/PeJ^{2}{}_{(i,j)}\right. \quad \ldots (15)$$

But, the stream function equation will be solved by relaxation method SOR as follows

$$l'_{(i,j)}\cdot\frac{\Psi_{(i+1,j)}-\Psi_{(i-1,j)}}{2\Delta x}+s'_{(i,j)}\cdot\frac{\Psi_{(i,j+1)}-\Psi_{(i,j-1)}}{2\Delta h}+a'_{(i,j)}\cdot\frac{\Psi_{(i+1,j)}-2\Psi_{(i,j)}+\Psi_{(i-1,j)}}{\Delta x^{2}}$$

$$+g'_{(i,j)}\cdot\frac{\Psi_{(i,j+1)}-2\Psi_{(i,j)}+\Psi_{(i,j-1)}}{\Delta h^{2}}-2b'_{(i,j)}\cdot\frac{1}{2\Delta x}\left(\frac{\Psi_{(i+1,j+1)}-\Psi_{(i+1,j-1)}}{2\Delta x}-\frac{\Psi_{(i-1,j+1)}-\Psi_{(i-1,j-1)}}{2\Delta h}\right)$$

$$+J^{2}{}_{(i,j)}.w_{(i,j)}=Error\approx 0 \quad \ldots(16)$$

The final form of stream function equation is

$$\Psi_{(IT+1)}=\Psi_{(IT)}+RF\ .\Delta\Psi_{(i,j)} \quad \ldots. (17)$$

**Calculation of Nusselt number**

When the solution convergence criterion is reached, the local and mean Nusselt numbers on the cylinder walls are calculated. From the balance of heat flux at the surface, the Nusselt number can be obtained as

$$Nu=-\frac{\partial q}{\partial n} \quad \ldots. (18)$$

Now, Equation (18) is transformed into general coordinate(ζ,η) as follows[21]:

$$Nu=\frac{1}{J\sqrt{g'}}\left[g'.q_h-b'.q_x\right] \quad \ldots. (19)$$

Since the temperature along the wall cylinder (w) is constant, $\frac{\partial q}{\partial x}=0$, Equation (19) becomes:

$$Nu=\frac{g'}{J\sqrt{g'}}q_h \quad \ldots(20)$$

The Nusselt number in Equation (20) is the local Nusselt number. To find the average Nusselt, the local Nusselt number should be integrated by using numerical integration [22].

**Results and Discussion**

The numerical solution of the steady flow over the cylinder is obtained for different free stream direction at Reynolds numbers of 20, 40, 100, 200, 300 and for parametric values of Grashof number in each case. It is found from the results that the velocity and temperature field is highly influenced by the free stream direction. Figure (2) shows the streamline contours for mixed convection around cylinder at Reynolds number (40) and (Gr =8000) with different free stream directions. In general, it can be seen from figure that the size and orientation of wake region are completely dependent on the free stream direction (λ) and ($Gr/Re^2$). No reverse flow takes place in the wake and the vortices completely disappear for ($\lambda = 0^o$, $45^o$ and $90^o$) and the flow separation at ($\gamma = 180^o$, $200^o$ and $210^o$) respectively. For opposing flow, the wake boundaries completely surround the cylinder forming a cylindrical dome. The circulation fluid inside the dome is driven by the buoyant forces and never gets entrained to the main stream. The separation occurs at stagnation point ($\gamma = 180^o$). Also, it is found that the temperature gradient decreases as (λ) increases [see Figure (3)]. This is due to the fact that, when ($\lambda = 0^o$), the buoyancy forces accelerate the flow, and the temperature gradient will increase. This effect will decrease as (λ) increase until reaching ($\lambda = 180^o$). On the other hand, at ($\lambda = 180^o$) the temperature gradient decreases. This is because, the circulating fluid in the wake is completely isolated from the main flow and heat is transferred from this region to the main flow by conduction across the wake

boundaries. Figure (4) shows the local Nusselt number distribution on the cylinder surface for case of Re = 100 and Gr = 50000 at different flow direction. In general, the local Nusselt number decreases over most of the cylinder surfaces as (λ) increases. This is expected to occur as a natural result of the slow down of the flow velocity near the cylinder surface. In assisting flow, the maximum Nusselt number occurs at stagnation point (γ =0).It is found that for ($\lambda \leq 135^o$), there is an increase in Nusselt number at ($\gamma = 230^o$, $265^o$ and $325^o$). This is due to the fact that at this location, the buoyancy forces aid the flow. It can be seen that for opposing flow, the maximum Nusselt number occurs at rare stagnation points ($\gamma = 0^o$ and $360^o$) and the minimum Nusselt number occurs near stagnation point. This is mainly because the buoyant forces aid the circulating flow close to the cylinder surface near ($\gamma = 0^o$ and $360^o$). This effect causes Nusselt number to increase with the increase of Grashof number in the same region, while a decrease in the region surrounding the forward stagnation point ($\gamma = 0^o$). It is found that the average Nusselt number decreases as (λ) increases. This is because the buoyancy forces aid the flow around most of cylinder surfaces, and this effect decreases as (λ) increases (see Figure (5)). A comparison with previous theoretical and experimental results as shown in figures (6 and 7).

**Correlation Equations**

It is usual to express the main governing variables by the way of putting a set of the correlation equations. These equations are responsible for the description of the whole results obtained.

The following equation is concerned with mixed convection around circular

$$\frac{\overline{Nu}}{\overline{Nu}_f} = 0.993\left[1 + (0.148 - 0.234\cos\lambda)\left(\frac{Gr}{Re^2}\right) + 0.00503\left(\frac{Gr}{Re^2}\right)^2\right]^{0.0304} \quad \ldots.(1)$$

The average Nusselt number for pure forced convection is correlated as

$$\overline{Nu}_f = 0.5145\ Re^{0.5} + 0.0004\ Re \quad \ldots..(2)$$

**Conclusions**

A numerical, finite – difference approach has been utilized for solving the governing equations for laminar, mixed convection around isothermal circular cylinder in cross flow. Results for local and average Nusselt number are obtained for Pr = 0.7 and ($0^o \leq \lambda \leq 180^o$). Ranges of Reynolds and Grashof numbers are (20 - 300) and (0-120000) respectively. From these results, the following conclusions can be drawn:

1. Free stream direction has a strong effect on the distributions of Nusselt number. The valuesofNusselt number decrease over most of the cylinder surfaces as (λ) increases.

2. For low value of Grashof number, the average Nusselt number decreases as(λ) increases. As Grashof number increases, the average Nusselt number increases monotonically for ($\lambda \leq 135^o$), while, the average Nusselt number decreases for ($\lambda > 135^o$) as Grashof number increases.

**References**

[1] Hatton ,A.P.,.James D.D.& Swire H.W., Combined Forced and natural Convection with low speed air fiow over hori –ontal cylinders , Fluid mech.,vol.42,pp.17-31,1970.

[2] Sharma,G., K.&Sukhatme,S., P., Combined Free and Forced Convection Heat Transfer From a Heated Tube to a transfer Air Stream , Transaction of the ASME , Journal of Heat Transfer , vol. 91,pp. 457 ,1969.

[3] Oosthuizen , P., H. &Madan, S., Combined Convective Heat Transfer From Hori-ontal Cylinders in Air ,Transactions of the ASME ,Joural of Heat Transfer .vol. 92, pp. 194- 196, 1970 .

[4] Oosthuizen , P., H. & Madam , S., The Effect of Flow Direction on Combined Convective Heat Transfer from Cylinders to Air , Transactions of the ASME , Journal of Heat Transfer , vol .93, pp. 240 – 242 , 1971 .

[5] Jackson , T., W. & Yen , H., H., Combined Forced and Free Convective Equations to Represent Combined Heat – Transfer Coefficients for a Hori- ontal Cylinder ,

Transction of the ASME ,Journal of Heat Transfer , vol.93, pp. 247- 248 , 1971 .

[6] Badr ,H., On the Effect of Flow Direction on Mixed Convection from a Hori=ontal Cylinder , International Journal for Numerical Methods in Fluids , vol . pp. 1-12, 1985 .

[7] Acrivos , A., On the Combined effect of Forced and Free Convection Heat Transfer in Laminar Boundary Layer Flows , Chemical Engineering Science , vol. 21 , pp. 343-352 ,1966.

[8] Joshi ,N., D . & Sukhatme , S., p., An Analysis of Combined Free and Forced Convection Heat Transfer From a Hori=ontal Circular Cylinder to a Transverse Flow , Transactions of the ASME ,XJournal of Heat Transfer , vol. 93, pp. 441-448,1971.

[9] Nakai , s., & Okazaki , T., Heat Transfer from Hori=ontal Wire at Small Reynolds and Grashof Numbers-II, International Joural of Heat and Mass Transfer ,vol.18, pp.397- 413,1975.

[10] Sparroww, E., M.& Lee, L., Analysis of Mixed Convection About a Hori=ontal Cylinder , International Journal of Heat and Mass Transfer , vol. 19, pp.229-231 , 1976.

[11] Merkin , J., Mixed Convection From a Hori=ontal Circular Cylinder , International Journal of Heat and Mass Transfer , vol. 20, pp.73 – 77 -,1977 .

[12] Jain , P., C. & Lohar , B., L., Unsteady Mixed Convection Heat Transfer from a Hori=ontal Circular Cylinder , Transactions of the ASME , Journal of Heat Transfer . vol. 101, pp. 126 -131 , 1979 .

[13] Badr , H., M., A Theoretical Study of Laminar Mixed Convection from a Hori=ontal Cylinder in Cross Stream , International Journal of Heat and Mass Transfer , vol. 26 , No. 5, pp. 639-653,1983.

[14] Badr , H., M., Laminar Combined Convection from a Hori=ontal; Cylinder – Parallel and Contra flow Regimes , International Journal of Heat and Mass Transfer , vol .27 , No. 1,pp. 15-27,1984.

[15] Armaly ,B., F., Chen, T., S. & Ramachandran , N., Correlations for Mixed Convection flows a Cross Hori=ontal Cylinders and spheres , Transactions of the ASME, Journal of Heat Transfer . vol. 110 , pp. 511-514 ,1988.

[16] Chang , K., S. & Jong , Y., Numerical Study of the Unsteady Mixed Convection HeatTransfer from a Circular Cylinder , International Comm .of Heat and Mass Transfer , vol. 16,pp. 427 -434 , 1989 .

[17] Chen ,C., K., Yang , Y.,T. &Sang , R., Laminar Mixed Convection from a Circular Cylinder Using a Body-Fitted Coordinate System , Journal of Thermo physics and Heat Transfer , vo;. 8, No. 4,pp.695-705 ,1994 .

[18] G.M.Laskowski ,S.P. Kearney , G. Evans and R. Greif , Mixed convection heat transfer to and from a horizontal cylinder in cross-flow with heating from below International Journal of Heat and Fluid Flow , July 2006

[19] A .A. van Steenhoven and C. C.M. Rindt, Flow transition behind a heated cylinder International Journal of Heat and Fluid Flow , Volume 24 , Issue 3 , June 2003 , Pages 322-333 .

[20] Jye , T., C., Wu , H.,W. &Huang , S., H., Heat Transfer Predictions around Three Heated Cylinders Between Two Parallel Plates , Journal of Numerical Heat Transfer ,Part A , vol .40, pp. 715 -733 ,2001 .

[21] Broughton , R., C. & Oliver , A., J., A Numerical Model for Convection in Complex – Dimensional Geometries and it is Application to Buoyancy flow in Power Cable, International Heat Transfer Conferences , vol . 2, pp. 447 – 451 , 1986 .

[22] AL- Khafaji , A., W. & Tooley ,J., R., Numerical Methods in Engineering Practice , Ist Edition ,CBS Publishing ,Japan Ltd , 1986 .

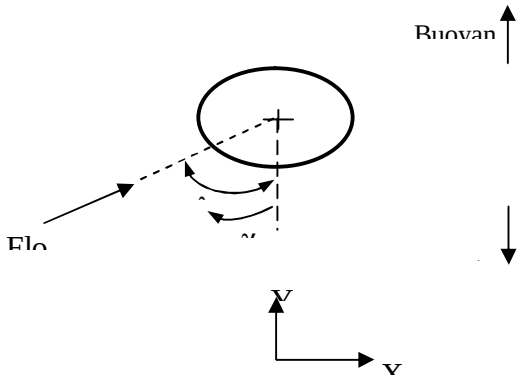


**Figure (1) Geometry and coordinate system for the present**

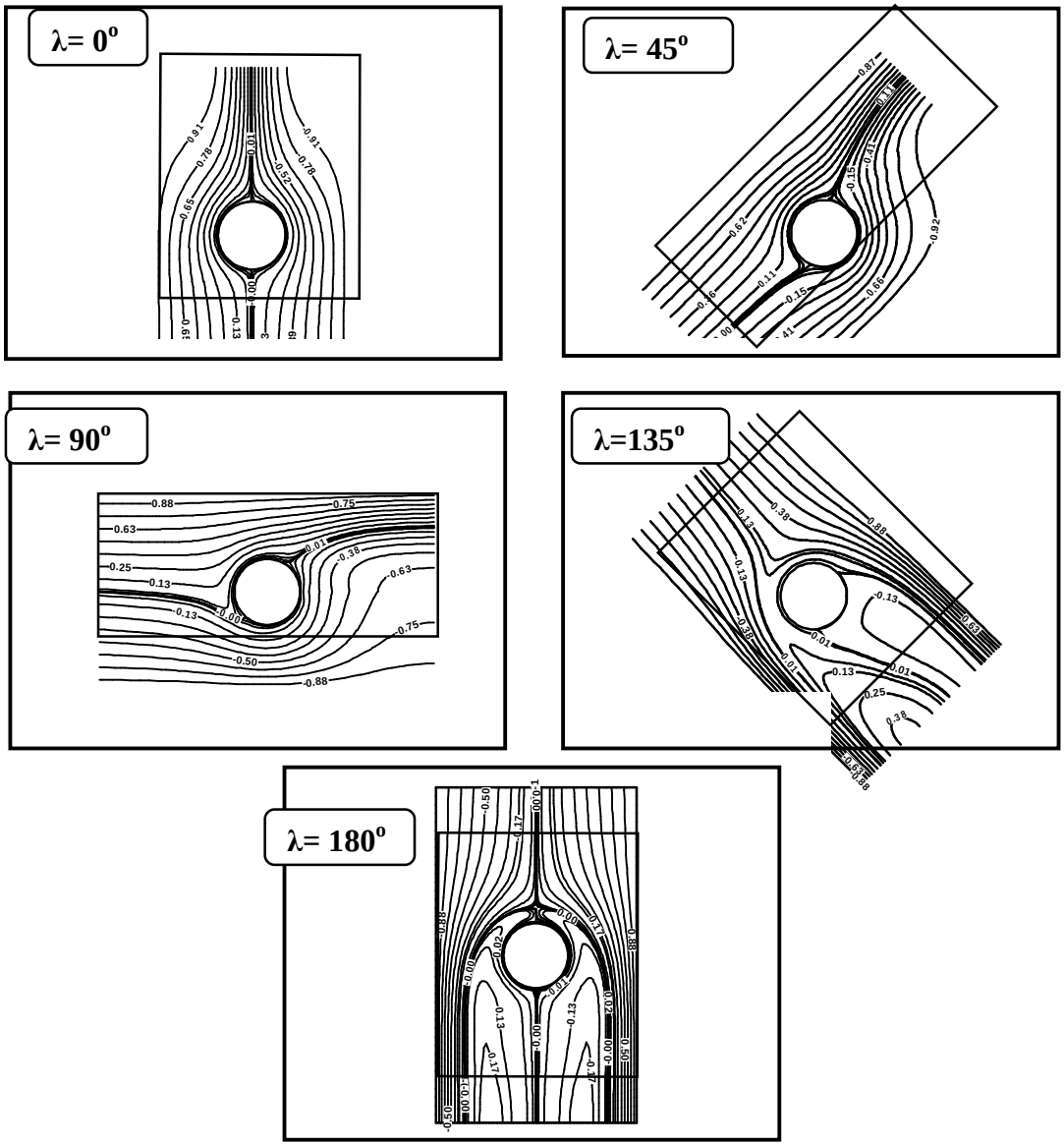


**Figure(2) Streamline contours for different free stream directions at Re = 40 and Gr =8000.**

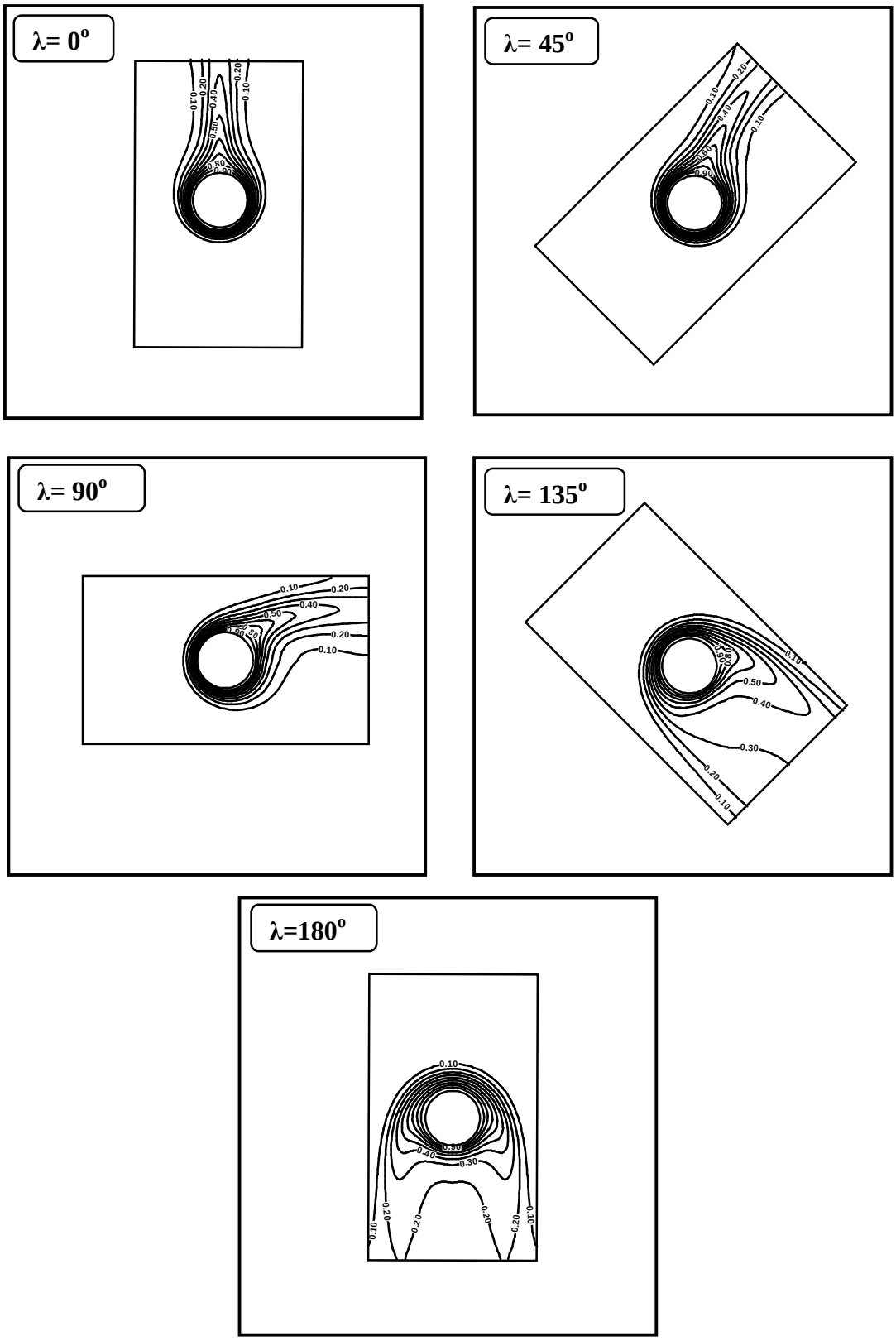


**Figure (3) Isotherm line contours for different free stream directions at Re = 40 and Gr =8000.**

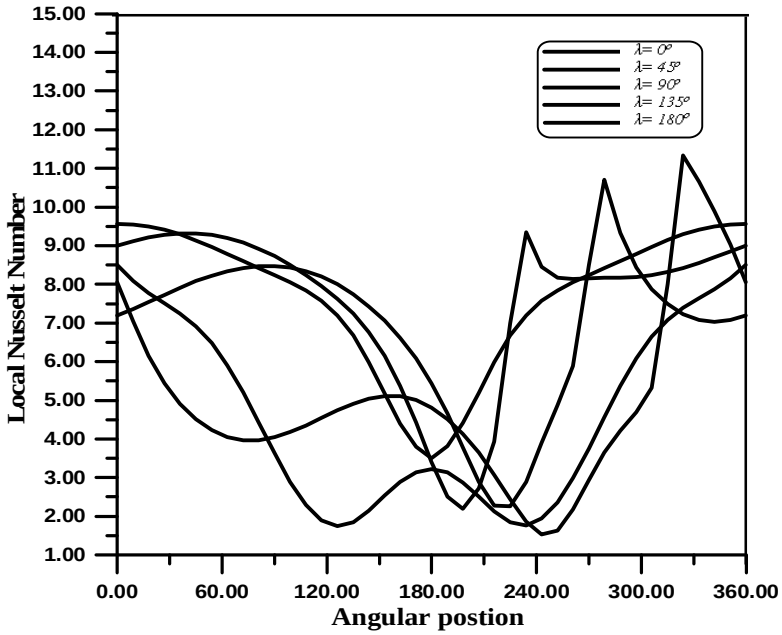


**Figure (4) Local Nusselt number distribution on the cylinder surface for different free stream directions at Re = 100 and Gr = 50000.**

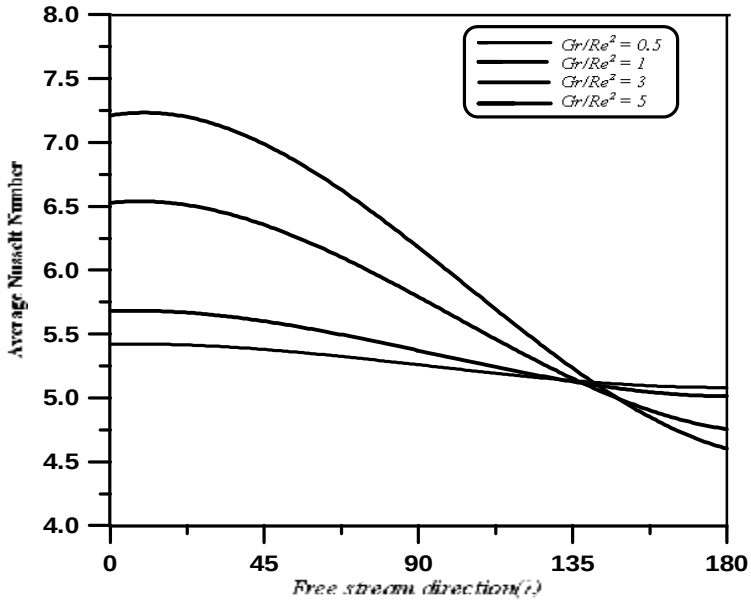


**Figure (5) Variation of average Nusselt number with free stream direction at Re = 40.**

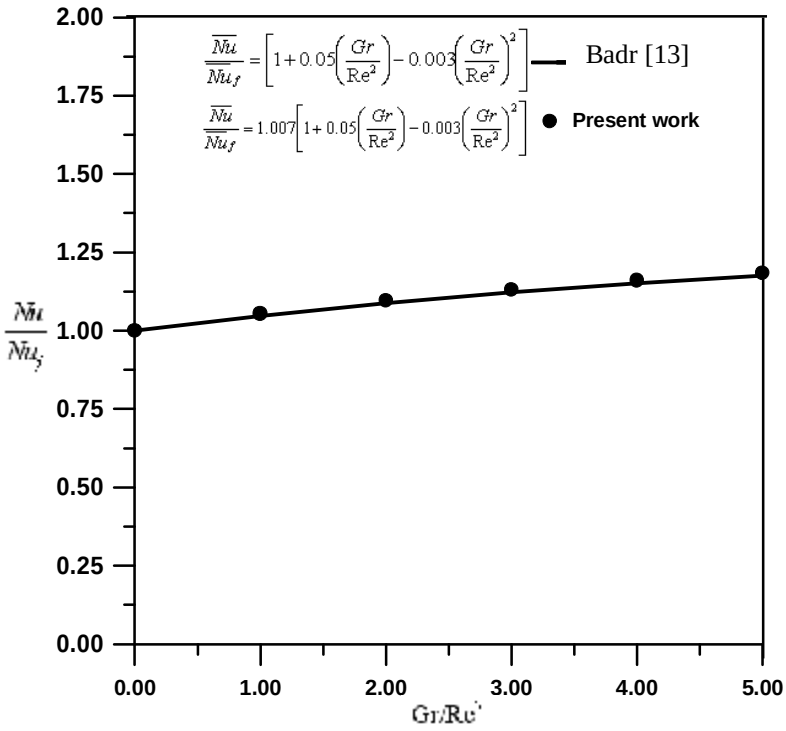


**Figure(6) Comparison between present work and theoretical result by Badr [13] at Re =100 and λ = 0°.**

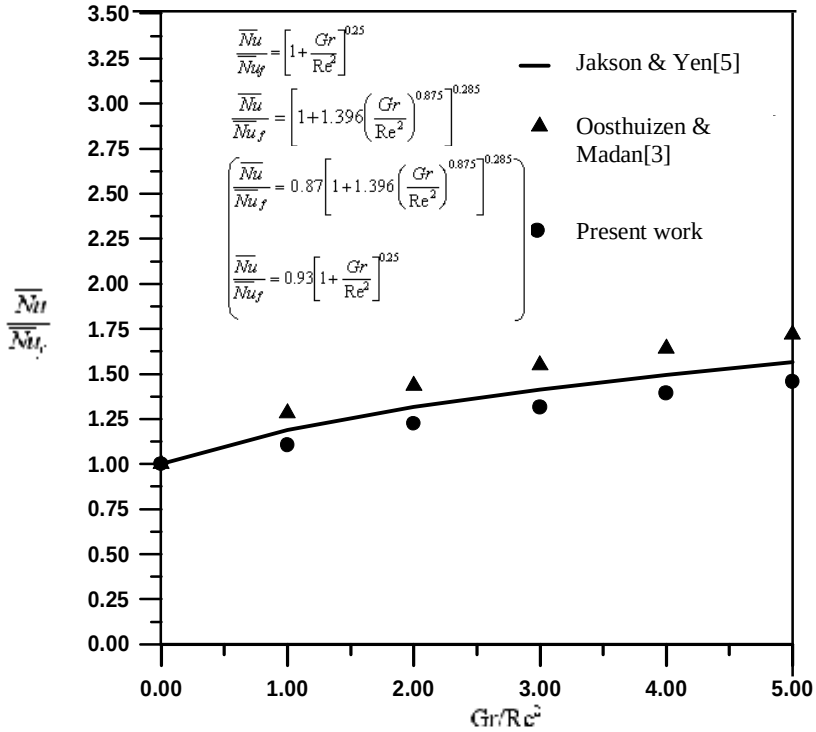


**Figure (7) Comparison between present work and previous experimental results at Re =100 and λ = 0°.**